Thermal properties analysis of BDK doped polymer optical fiber gratings

YANHUA LUO[a,b,*], WENXUAN WU[a], XUSHENG CHENG[c], XIN WANG[a], XIUJIE TIAN[a], TONGXIN WANG[a], QIJIN ZHANG[a] , GANG-DING PENG[b], BING ZHU[c]

[a]*CAS Key Laboratory of Soft Matter Chemistry, Department of Polymer Science and Engineering, University of Science and Technology of China, Key Laboratory of Optoelectronic Science and Technology, Anhui Province, Hefei, Anhui 230026, China*

[b]*School of Electrical Engineering, University of New South Wales, Sydney 2052, NSW, Australia*

[c]*Department of Electronic Engineering and Information Science, University of Science and Technology of China, Hefei, Anhui 230026, China*

To know more about the thermal properties of benzil dimethyl ketal (BDK) doped polymer optical fiber (POF) gratings, differential thermal analysis, thermal mechanical analysis, thermal optical analysis and thermal response analysis were performed. The results show that the maximum working temperature of such POF gratings is around 81.7^{o}C. This POF expands after heating till it reaches 80.0^{o}C and then thrinks. The linear thermal expansion coefficient of POF is around 78.51×10^{-6} /^{o}C from 25.4 to 80.0 ^{o}C. The thermal optic coefficient is -1.73×10^{-4} /^{o}C. Furthermore, the sensitivity of such POF gratings is around -147 pm/^{o}C at the temperature region from 24^{o}C to 52^{o}C. All these results offer the direction to tailor the BDK-doped POF gratings for temperature sensing, especially for temperature sensing in-vivo.

(Received May 6, 2012; accepted September 20, 2012)

Keywords: Polymer optical fiber gratings, Temperature sensor, Thermal properties, Thermal expansion, Thermal-response,

1. Introduction

POFs have shown great potential to sense temperature and strain with higher sensitivity and wider tunability than its silica counterpart [1], in addition, they are clinically acceptable, flexible and non-brittle making them important candidates for in-vivo biosensing applications [2-9]. For sensing application, POF grating is one of the most active fields. Since its first fabrication in 1999 [10], POF gratings have been fabricated with different fiber structure, different materials and different writing method and used in a series sensing field [11-24].

POF gratings have higher temperature sensitivity, because of large thermo-optic coefficient and large thermal expansion coefficient of polymers [11, 18, 20, 25, 26], Therefore, the refractive index or physical length of POF gratings are generally much more sensitive to temperature than those of silica, more than 10 times of the silica fiber gratings [27, 28]. For a given change of temperature, temperature sensors of POF gratings show a much greater wavelength shift than their silica counterparts, either allowing the use of lower resolution, simpler and therefore cheaper interrogation systems or alternatively enabling the sensors to be used in demanding applications, for example temperature sensing *in vivo*. In addition, the high temperature sensitivity of POF based devices allows device properties to be readily controlled thermally [29]. Moreover, advantage could be taken of the fact by making use of the huge range of organic chemistry techniques to modify the fiber materials [29] as well as lots of mechanical method or design to modify the fiber structure [25, 26, 30, 31].

So far, the temperature sensitivity of the gratings in the step index poly(methyl methacrylate) (PMMA) based POFs has been studied previously [25, 26, 32], revealing a negative temperature coefficient of between -146 pm/°C and -360 pm/°C significantly larger in magnitude than that observed for fiber Bragg gratings (FBGs) in silica fibers, which is around 10 pm/°C [28]. However, Chen et al found that temperature response of PMMA POF with an eccentric core shows a negative sign with the thermal sensitivity of −50.1 pm/^{o}C [30]. And in PMMA microstructured optical fibers (mPOFs), Karen E Carroll et al found a lower magnitude of temperature sensitivity between -52 pm/°C and -95 pm/°C [28], where there exists a complex thermal response of Bragg gratings in PMMA mPOFs due to its organic nature [28, 29, 33]. For Bragg gratings created in perfluorinated cyclic transparent optical polymer (CYTOP) POF, the temperature sensitivity is nearly -167 pm/^{o}C [34]. For the FBGs in TOPAS® cyclic olefin copolymers (TOPAS) mPOF, there is a calculated largest positive temperature sensitivity of 810 pm/°C [31]. Recently, negative temperature sensitivity in TOPAS FBG in mPOF operating at 870nm has also been realized to be -60 pm/^{O}C [22]. All these work demonstrates that the thermal response of POF gratings has great dependence upon their materials, fiber structure, fabrication process, temperature range, etc. [22, 25, 26, 28-34]

In our previous work, we have reported a high-sensitivity temperature sensor based on Bragg grating in BDK-doped PMMA photosensitive POF with a

temperature sensitivity of -149 pm/◦C [32]. Therefore, a more extensive study is required for practical application of the BDK doped POF gratings into temperature sensing field. In this paper, the operating temperature, thermal expansion, thermal optic and thermal response properties of BDK doped POF and POF gratings have been studied, which provide an effective reference for BDK-doped photosensitive POF gratings used as a temperature sensor.

2. Experiments

2.1 POF fabrication

POF doped with BDK was fabricated according to the previous report [35]. Fiber parameters and grating fabrication conditions are listed in Table 1

Table 1 . Description of Grating Fabrication Process.

POF Specification	Grating Fabrication Process
Cladding(methyl methacrylate(MMA):ethyl methacrylate(EMA) = 60:40 v%) Core(MMA:EMA: benzyl methacrylate (BzMA):BDK = 50:45:3:2 v%) $n_{co} - n_{cl}$: ~ 0.001(633nm) n_{cl}: ~ 230μm n_{co}: ~ 11 μm	355nm frequency-tripled Nd:YAG pulse laser Frequency: 10 Hz Pulse width: 6 ns Average power intensity:57mW/cm^2 Grating length: 6 mm Phase mask period: 1.0614um

2.2 POF gratings fabrication

According to the previous work [14], POF gratings were fabricated in a short part of photosensitive POF doped with BDK with sagnac ring system. After 2 min 57 mW/cm^2 355 nm illumination, the reflection spectrum of FBGs formed as shown in Fig. 1. The Bragg wavelength is around 1571.8 nm, the reflection intensity is about 3.7 dB above the noise level, and full width at half maximum (FWHM) is about 0.22 nm. Furthermore, the effective refractive index of the core could be deduced about 1.481.

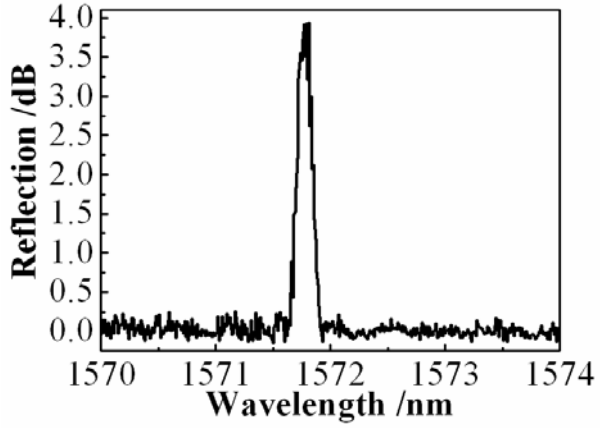

Fig. 1. The reflection spectrum of FBGs in POF doped with BDK after 2 min 355 nm UV exposure.

2.3 General Measurements

Differential scanning calorimetry (DSC) was performed with a Perkin Pyris-1 DSC under nitrogen atmosphere (heating rate: 10 °C/min), while thermo mechanical analysis (TMA) was performed with a Netzsch DIL-402C (1600 ℃model) under air atmosphere (heating rate: 5.00 °C/min).

2.4 Thermal-optic response of POF gratings

The thermal response of POF gratings was performed with the experimental setup shown in Figure 2. Both ends of POF with Bragg gratings were fixed using epoxy glue vertically on a metal panel. Then the sensing part of POF gratings was put into the oven and temperature was controlled by the PID method, where the accuracy of the temperature measurement was ±1°C. And it took about 2 min for the heating system to reach the desired temperature and 5 min for the stabilizing of the temperature. The reflection spectra of the POF Bragg gratings were measured by an optical spectrum analyzer (OSA) when the thermal test was performed. A tunable laser source was adopted for the POF Bragg grating characterization, launched into the POF through a 3dB Y-type silica fiber coupler.

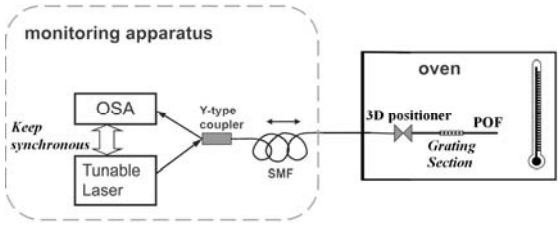

Fig. 2. The experiment setup for the test of the thermal response of POF gratings.

3. Theory analysis of POF gratings thermal response

According to Bragg condition, the central reflected wavelength has the following relationship with the grating period (Λ) and the effective refractive index of guide mode (n_{eff}) [36]:

$$\lambda_B = 2n_{eff}\Lambda \tag{1}$$

From Eq. (1), when the optical fiber gratings take the temperature changes only, thermal-optic effects cause the change of n_{eff} (close to the core index) and the thermal expansion effects cause the change of grating period Λ. So the Bragg wavelength λ_B will change. If we regard Bragg wavelength λ_B as the function of temperature T, we can open $\lambda_B(T)$'s Taylor progression [36]:

$$\lambda_B(T) = \lambda_B(T_0) + 2\left(n_{eff}\frac{\partial\Lambda}{\partial T} + \Lambda\frac{\partial n_{eff}}{\partial T}\right)_{T_o}\Delta T + 2\left(n_{eff}\frac{\partial^2\Lambda}{\partial T^2} + \Lambda\frac{\partial^2 n_{eff}}{\partial T^2}\right)_{T_o}(\Delta T)^2 + \ldots\ldots \tag{2}$$

When ΔT is not very large, high-order item which is higher than $(\Delta T)^2$ can be ignored. In addition, we define $\alpha = \frac{1}{\Lambda}\cdot\frac{\partial\Lambda}{\partial T}$ and $\zeta = \frac{1}{n_{eff}}\cdot\frac{\partial n_{eff}}{\partial T}$ as core's linear thermal expansion coefficient and thermal-optic coefficient. So we can predigest Eq. (2) [36]:

$$\Delta\lambda_B(T) = 2(\alpha+\zeta)n_{eff}\Lambda\Delta T \tag{3}$$

Combining Eqs. (1) and (3), we could get the following form:

$$\frac{\Delta\lambda_B}{\lambda_B} = (\alpha+\zeta)\Delta T \tag{4}$$

Due to Eq. (4), when POF gratings were affected by temperature only, $\frac{\Delta\lambda_B}{\lambda_B}$ and ΔT became linear relation. So the coefficient can be obtained conveniently by measuring the relative shift of the Bragg wavelength $\frac{\Delta\lambda_B}{\lambda_B}$ and the change of the temperature ΔT, which is the sum of FBG's thermal expansion coefficient and thermal-optic coefficient. The FBG's thermal response coefficient is dependent upon the thermal-mechanical and thermal optic properties. The thermal expansion and thermo-optic properties of the material decides the Bragg wavelength shift directions. Therefore , it is valuable and necessary to do the thermal-mechanical and thermal optic properties study for the POF gratings.

4. Result and discussion

4.1 Differential thermal analysis

As one kind of the polymer materials, POF gratings should be operating under the glass transition temperature if good repeatability and stability is desired. Therefore, DSC of a section of the POF was measured as shown in Fig. 3. Fig. 3 displays DSC heating curves during heating process. Seen from DSC curve, there is a small phase transition at 48.2 °C, which may be attributed to the disturbing orientation of the main chain of POF materials. When the optical fiber is drawn from POF preform, the main chain of the polymer has the orientation to some extent [37, 38]. When heating the POF, the orientation will be relaxed due to thermal motion, which will absorb the heat. The heat content is around 0.0488 J/(g·°C). Therefore, to assure the stability and repeatability of such POF gratings temperature sensor [39], the fiber prior to grating inscription should be annealed a little higher than 48.2 °C. It may also explain the thermal response transition almost without measurable change in density in [20].

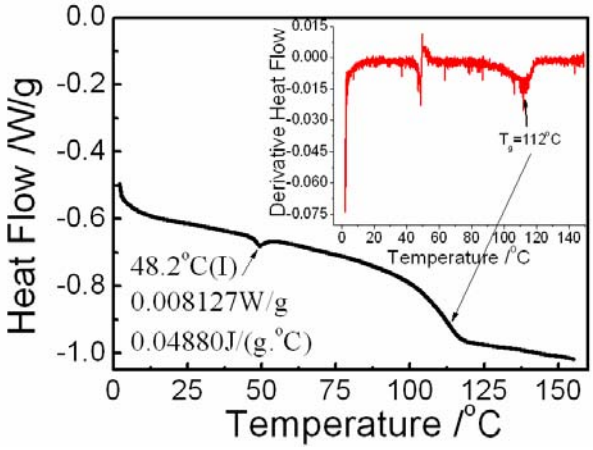

Fig. 3. BDK-doped POF of differential thermal analysis curves, heating rate of 10 °C / min, under the nitrogen atmosphere, and the illustration is the differential thermal analysis curves of the derivative curve.

Then at beginning of 81.7 °C, the curve decrease faster, till it reaches 116.7 °C, which shows glass transition of POF materials around 112 °C seen from the inset of the Fig. 3, similar to the value reported before [40]. That means from 81.7 °C, POF changed from the brittle to ductile and which was invoked as a possible explanation for the change in cleaving behaviour with temperature reported by Law *et al* [41]. For POF gratings, the movement of polymer chain will become more severe and finally the gratings written in the core will disappear. In addition, POF can be cleaved well with the hotplate temperature higher than 81.7 °C. This transition temperature is dependent on the thermal history of the fiber, as well as the fiber drawing parameters [37] and UV exposure [42]. Therefore, the maximum operating temperature of such POF gratings should be lower than 81.7 °C. Furthermore, according to the literature [40], the degradation temperature of POF is around 282 °C, which may be taken as an upper limit operating temperature of POF gratings.

4.2 Thermal mechanical analysis

In order to know better the thermal-mechanical property of the POF gratings, the thermal mechanical

analysis of a section of POF with 11mm length was performed on Netzsch DIL 402 C (1600 ℃ model). The result was shown in Figure 4, which displays TMA curve during heating process. Seen from TMA curve, from 25.4 to 80.0 °C, the dimension increases from 0 to 45.83 μm, showing that POF expands after heating. Through the linear fitting, from 25.4 to 80.0 °C, the linear thermal expansion coefficient of POF is around 78.51×10^{-6} /°C. After 80.0 °C, the dimension changes and starts to decreases. The dimension changes from positive to negative value, which means that POF starts shrinking. Combining the result of the differential thermal analysis, it shows that when the temperature increased to the glass transition temperature, the POF starts to shrink as POF is drawn from POF preform, when the temperature is higher than T_g, the movement of polymer chain become stronger and easier, and finally the polymer chain in POF will collapse, so the POF will shrink. Compared with the previous work [28], there was a threshold temperature for POF gratings. When heating temperature is above this point, a permanent blue shift in the Bragg wavelength will occur. The threshold temperature is dependent on the thermal history of the POF gratings, which should be due to shrinking of the polymer fiber [30] as described above. In addition, it can also be clearly to explain why the POF gratings can not survive up or higher than 100 °C [28].

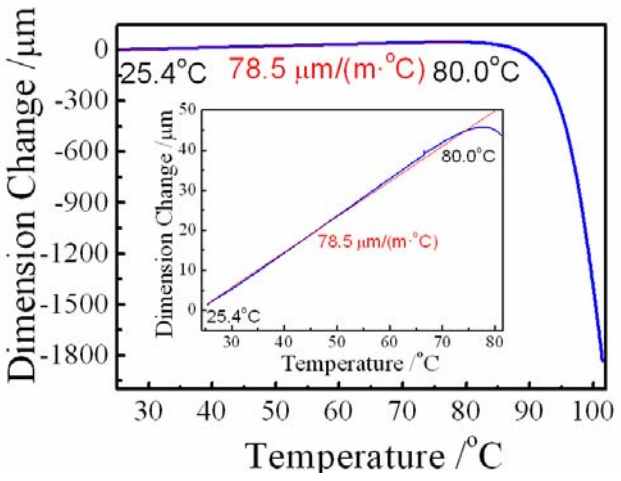

Fig. 4 BDK-doped POF of thermal mechanical analysis curves, heating rate of 5 °C / min.

4.3 Thermal optical analysis

It is known that the change in refractive index n of a polymer with temperature is due to the temperature-caused density change and temperature change itself as [43]. According to [44], the relationship between the thermal-optic coefficient (dn/dT) and the volume coefficient of thermal expansion of a polymer (α) satisfy the following empirical equation:

$$\frac{dn}{dT} = -0.56\gamma - 3.7\times10^{-6} \quad (5)$$

where the volume coefficients of thermal expansion (γ values) of the polymers are three times of the linear coefficient values (α values) that were directly obtained from the TMA measurement ($\gamma = 3\alpha$). Since the above empirical equation comes from diverse chemical structure of polymers, it is suggested that the relationship be reasonably extended to the other types of polymers/materials as an empirical equation [44]. Seen from the Eq. (5), with the temperature increasing, the refractive index of the POF core materials decreases. Due to the thermal-optic coefficient of the main composition of POF are copolymer of MMA and EMA, whose thermal-optic coefficients of polymers are -1.3×10^{-4} /°C and -1.1×10^{-4} /°C, respectively [44]. Due to the lower concentration of 2 v% BDK doped and 3 v% BzMA of co-polymerized, the thermal-optic coefficient should have a little difference but can not be too large due to the small content of them [45]. In addition, regardless the difference with core and cladding, since the coefficients of thermal expansion (α) of POF has already been measured using TMA, such an empirical equation can give out the the dn/dT values of POF, which is about -1.36×10^{-4} /°C close to the value of the base material PMMA [44]. Furthermore, ζ can be calculated, which is around -0.92×10^{-4} /°C.

4.4 Thermal response analysis

Finally , the thermal response of POF gratings from 24 °C to 52 °C, which covers the in-vivo temperature region, was measured using the setup shown in Fig. 2, and the result of the thermal response is shown in Fig. 5(A). Like the report before [25, 26], below a transition temperature the Bragg wavelength decreases linearly and POF gratings based on PMMA display a negative wavelength shift with rising temperature [26]. It can be fitted with the following equation:

$$\lambda_B = 1571.846 - 0.147T \quad (6)$$

From Eq. (6), the sensitivity of this POF gratings used for temperature sensing can be obtained, which is around -147 pm/°C, 10 times larger than the silica gratings, in accordance with the previous report [34]. It can be seen that almost 4 nm tuning range can be achieved only with the temperature variation of 28 °C, which is larger than the few nanometers achieved in silica fiber grating by the several hundred degree temperature variation [46]. This can also indicate that POF gratings have higher thermal sensitivity than silica fiber Bragg gratings and show great potential used as a temperature sensor.

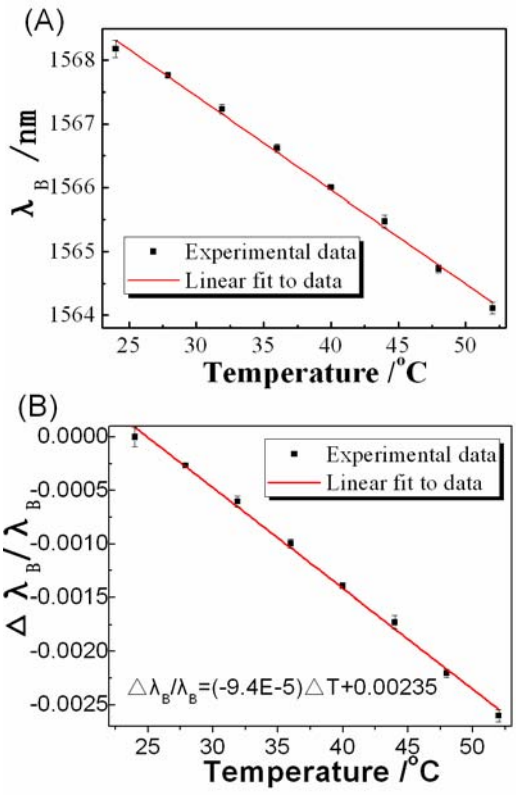

Fig. 5. (A) Bragg wavelength of POF Bragg gratings vs temperature, and (B) the relative shift of Bragg wavelength of POF gratings vs temperature.

Furthermore, the relative shift of Bragg wavelength of POF gratings vs temperature can be obtained as shown in Fig. 5(B). According to Eq. (4), the experiment data could be linearly fitted with the following equation:

$$\frac{\Delta\lambda_B}{\lambda_B} = 0.00235 - 9.4\times10^{-5}\Delta T \qquad (7)$$

From Eq. (7), the thermal coefficient of the POF gratings can be obtained which is about -9.4×10^{-5} °C, far larger than silica fiber gratings ($7.5\times10^{-6}/^{o}C$) [47]. In addition, it could be assumed that the thermal expansion coefficient of the core materials is almost the same as the POF as the difference of the core and cladding materials are similar and the core and cladding are continuous. So the thermal expansion coefficient of the core could be taken as 78.51×10^{-6} °C, and the thermal optic coefficient can be calculated to be -1.73×10^{-4} °C from Eq. (4), which is very close to the value reported in the literature [48], but smaller than the value calculated from the empirical equation.

5. Conclusion

To have a good use of BDK-doped photosensitive POF gratings as a temperature sensor, the thermal properties was investigated. The POF used should be annealed a little higher than 48.2 °C to assure the stability and repeatability of such POF gratings temperature sensor. The maximum operating temperature of such POF gratings should be lower than 81.7 °C. POF expands after heating till it reaches 80.0 °C and then thrinks. The linear thermal expansion coefficient of POF is around 78.51×10^{-6} /°C from 25.4 to 80.0 °C. The thermal optic coefficient is -1.73×10^{-4} °C. The sensitivity of such POF gratings is around -147 pm/°C, very favorably compared with the typical value of 10 pm/°C for FBGs in silica fiber, showing great potential as a high sensitive temperature sensor. All these results provide an effective reference for the BDK-doped photosensitive POF gratings as a temperature sensor.

Acknowledgement

The authors gratefully acknowledge the financial support by National Natural Science Foundation of China (No. 21074123 , 91027024 and 50973101), an International Science Linkages (ISL) Australia China Special Fund (CH060036) from the Department of Industry, Innovation, Science and Research (DIISR), Australia and Open Fund of State Key Laboratory of Information Photonics and Optical Communications (Beijing University of Posts and Telecommunications) and wish to express their thanks to the referees for critically reviewing the manuscript and making important suggestions.

References

[1] A. Stefani, W. Yuan, C. Markos, O. Bang, IEEE Photon. Technol. Lett. **23**, 660 (2011) .
[2] G. Emiliyanov, J. B. Jensen, O. Bang, P. E. Hoiby, L. H. Pedersen, E. M. Kjær, Opt. Lett. **32,** 460 (2007).
[3] G. Emiliyanov, J. B. Jensen, O. Bang, P. E. Hoiby, L. H. Pedersen, E. M. Kjær, Opt. Lett. **32**, 1059 (2007).
[4] G. E. Town, W. Yuan, R. McCosker, O. Bang, Opt. Lett. **35**, 856 (2010).
[5] C. Markos, W. Yuan, K. Vlachos, G. E. Town, O. Bang, Opt. Express **19**, 7790 (2011).
[6] W. Yuan, G. E. Town, O. Bang, IEEE Sens. J. **10**, 1192 (2010).
[7] F. M. Cox, A. Argyros, M. C. J. Large, Opt. Express **14**, 4135 (2006).
[8] J. Jensen, P. Hoiby, G. Emiliyanov, O. Bang, L. Pedersen, and A. Bjarklev, Opt. Express **13,** 5883 (2005).
[9] A. Dupuis, N. Guo, Y. Gao, N. Godbout, S. Lacroix, C. Dubois, M. Skorobogatiy, Opt. Lett. **32**, 109 (2007).
[10] G. D. Peng, Z. Xiong, P. L. Chu, Opt. Fiber Technol. **5**, 242 (1999).

[11] J. M. Yu, X. M. Tao, H. Y. Tam, Opt. Lett. **29**, 156 (2004).
[12] Z. C. Li, H. Y. Tam, L. X. Xu, Q. J. Zhang, Opt. Lett. **30,** 1117 (2005) .
[13] H. Dobb, D. J. Webb, K. Kalli, A. Argyros, M. C. J. Large, M. A. v. Eijkelenborg, Opt. Lett. **30**, 3296 (2005).
[14] Y. H. Luo, Q. J. Zhang, H. Y. Liu, G. D. Peng, Opt. Lett. **35**, 751 (2010).
[15] Z. F. Zhang, C. Z., X. M. Tao, G. F. Wang, G.-D. Peng, IEEE Photon. Technol. Lett. **22**, 1562 (2010).
[16] X. Chen, C. Zhang, D. J. Webb, R. Suo, G. D. Peng, K. Kalli, Proc. SPIE **7503**, 750327-1-4 (2009).
[17] I. P. Johnson, D. J. Webb, K. Kalli, M. C. J. Large, A. Argyros, Proc. SPIE **7714**, 77140D-1-10 (2010).
[18] H. Y. Liu, H. B. Liu, G. D. Peng, and P. L. Chu, Opt. Commun. 266 (2006) 132-135.
[19] C. Zhang, X. Chen, D. J. Webb, G.-D. Peng, Proc. SPIE **7503**, 750380-1-4 (2009).
[20] D. J. Webb, K. Kalli, C. Zhang, M. Komodromos, A. Argyros, M. Large, G. Emiliyanov, O. Bang, E. Kjaer, Proc. SPIE **6990**, 69900L-1-10 (2008).
[21] C.C. Ye, J.M. Dulieu-Barton, D.J. Webb, C.Zhang, G.-D. Peng, A. R. Chambers, F. J. Lennard, D.D.Eastop, Proc. SPIE **7503**, 75030M-1-4 (2009).
[22] W. Yuan, L. Khan, D. J. Webb, K. Kalli, H. K. Rasmussen, A. Stefani, and O. Bang, Opt. Express **19**, 19731 (2011) .
[23] I. P. Johnson, D. J. Webb, K. Kalli, Proc. SPIE **8351**, 83510M-1-8 (2012).
[24] W. Yuan, A. Stefani, O. Bang, IEEE Photon. Technol. Lett. **20**, 401 (2012).
[25] H. Y. Liu, H. B. Liu, G. D. Peng, P. L. Chu, Opt. Commun. **219**, 139 (2003).
[26] H. Y. Liu, G. D. Peng, P. L. Chu, IEEE Photon. Technol. Lett. **13**, 824 (2001).
[27] G. D. Peng, P. L. Chu, Proc. SPIE **4929**, 303 (2002).
[28] K. E. Carroll, C. Zhang, D. J. Webb, K. Kalli, A. Argyros, M. C. J. Large, Opt. Express **15**, 8844 (2007).
[29] H. Dobb, K. Carroll, D. J. Webb, K. Kalli, M. Komodromos, C. Themistos, G. D. Peng, A. Argyros, M. C. J. Large, M. A. van Eijkelenborg, Q. Fang, I. W. Boyd, Proc. SPIE **6189**, 618901-1-12 (2006).
[30] X. Chen, C. Zhang, D. J. Webb, G.-D. Peng, K. Kalli, Meas. Sci. Technol. **21**, 094005 (2010).
[31] D. J. Webb, K. Kalli, K. Carroll, C. Zhang, M. Komodromos, A. Argyros, M. Large, G. Emiliyanov, O. Bange, E. Kjaer Proc. SPIE 6830, 683002-1-9 (2007).
[32] X. Cheng, W. Qiu, W. Wu, Y. Luo, X. Tian, Q. Zhang, B. Zhu, Chin. Opt. Lett. **9**, 020602 (2011).
[33] H. Dobb, K. Carroll, D. J. Webb, K. Kalli, M. Komodromos, C. Themistos, G. D. Peng, A. Argyros, M. C. J. Large, M. A. v. Eijkelenborg, M. Arresy, S. Kukureka, Proc. SPIE **6193**, 61930Q-1-12 (2006).
[34] H. Y. Liu, G. D. Peng, P. L. Chu, Opt. Commun. **204**, 151 (2002).
[35] W. Wu, Y. Luo, X. Cheng, X. Tian, W. Qiu, B. Zhu, G. D. Peng, Q. Zhang, J. Optoelectron. Adv. Mater. **12**, 1652 (2010).
[36] J. Ye, B. Peng, J. Fang, T. Huang, Y. Liao, M. Zhang, Proc. SPIE **6279**, 627961-1-16 (2007).
[37] T. Ishigure, M. Hirai, M. Sato, Y. Koike J. Appl. Polym. Sci. **91**, 404 (2004).
[38] M. Sato, M. Hirai, T. Ishigure, Y. Koike, J. Lightwave Technol. **18**, 2139 (2000).
[39] W. Yuan, A. Stefani, M. Bache, T. Jacobsen, B. Rose, N. Herholdt-Rasmussen, F. K. Nielsen, S. Andresen, O. B. Sørensen, K. S. Hansen, O. Bang, Opt.Commun. **284**, 176 (2011).
[40] D. X. Yang, J. Xu, X. Tao, H. Tam, Mater. Sci. Eng. A **364**, 256 (2004) -259.
[41] S. H. Law, J. D. Harvey, R. J. Kruhlak, M. Song, E. Wu, G. W. Barton, M. A. v. Eijkelenborg, M. C. J. Large, Opt. Commun. **258**, 193 (2006).
[42] E.E. Shafee, Polym. Degrad. Stabil. **53**, 57 (1996).
[43] M. B. J. Diemeer, Opt. Mater. **9**, 192 (1998).
[44] Z. Zhang, P. Zhao, P. Lin, F. Sun, Polymer **47**, 4893 (2006).
[45] G. V, N. RO, S. S, and S. BJ., eds., Physical properties of polymers handbook (AIP Press, Woodbury, 1996), p. 535.
[46] K. O. Hill and G. Meltz, J. Lightwave Technol. **15**, 1263 (1997).
[47] H. Jia, Theoretical and technical researches on the optical fiber grating sensors, (Xi'an Optics and Fine Mechanics, Chinese Academy of Sciences, 2000) PhD thesis.
[48] E.-S. Kang, T.-H. Lee, and B.-S. Bae, Appl. Phys. Lett. **81**, 1438 (2002).

*Corresponding author: yhluo3@mail.ustc.edu.cn